ELSEVIER

Volume 181, Number 7, July 2008

Special Issue: Solid State Chemistry on the Nanoscale: Achievements, Challenges, and Opportunities

Guest Editor: Prof. Raymond E. Schaak

JOURNAL OF SOLID STATE CHEMISTRY

www.elsevier.com/locate/jssc

# CONTENTS

Abstracted/indexed in BioEngineering Abstracts, Chemical Abstracts, Coal Abstracts, Current Contents/Physics, Chemical, & Earth Sciences, Engineering Index, Research Alert, SCISEARCH, Science Abstracts, and Science Citation Index. Also covered in the abstract and citation database SCOPUS®. Full text available on ScienceDirect®.

## *Editorial*



## *Review*



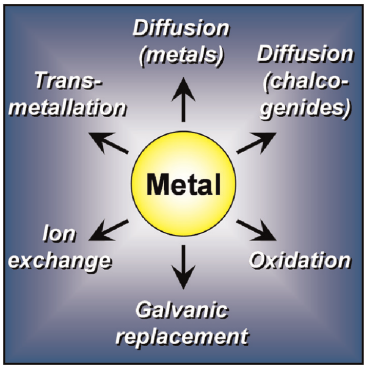


Nanocrystal conversion chemistry uses pre-formed nanoparticles as templates for chemical transformation into derivative solids, helping to define the composition, crystal structure, and morphology of product nanocrystals that have more complex features than their precursor templates. This article highlights the application of this concept to diverse classes of solids, including metals, oxides, chalcogenides, phosphides, alloys, intermetallics, sulfides, and nitrides.

## *Regular Articles*



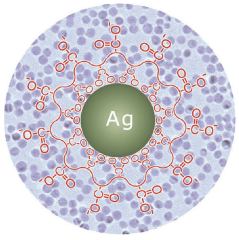


Silver nanocrystals with uniform and controllable sizes (<20 nm) have been synthesized using a modified polyol process. The use of polyacrylic acid as the surfactant significantly limits the nanocrystal growth, prevents the interparticle aggregation and fusion, and leads to a uniform population of samples with high water solubility.



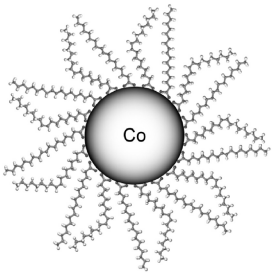


Magnetic Co nanoparticles were synthesized in the presence of different capping agents and the effect of their molecular structures on the morphology of Co nanoparticles was analyzed. The transformation between cis- and trans-isomers of olefinic acids was critical to the formation of a densely packed monolayer on the surface of small nanoparticles characterized by high curvatures.

## *Regular Articles—Continued*



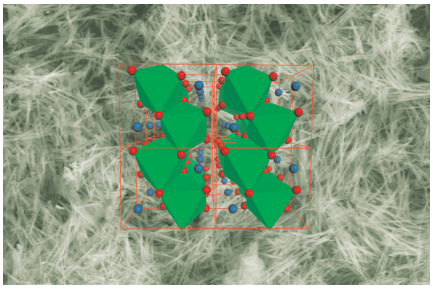

Systematic synthesis of crystalline, multiferroic MnWO4 nanowires and nanowire arrays with controllable chemical composition and morphology, using a modified template-directed methodology under ambient room-temperature conditions.

---



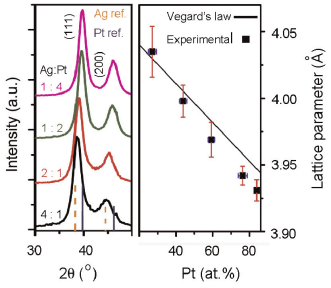


While platinum and silver cannot form a solid solution with the composition between about $Ag_2Pt_{98}$ and $Ag_{95}Pt_5$ at 400 °C or below in bulk form, alloy particles and wires can be made within this miscibility gap at the nanometer scale.

---



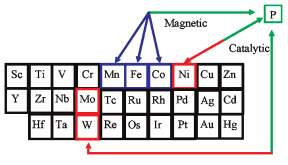


Recent advances in synthetic methods have led to the preparation of a wide array of transition metal phosphide nanoparticles, and characterization of these materials has provided insight into nanoscale magnetic and catalytic properties. This paper highlights advances in the field that have been made since 2004.



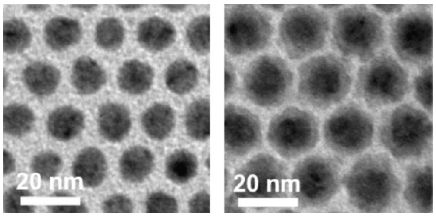


The 10 nm/3 nm Co/$MFe_2O_4$ ($M$ = Fe, Mn) bimagnetic core/shell nanocomposites are synthesized from the surface coating of ferrite shell over 10 nm Co nanoparticle seeds. The nanocomposites show much enhanced chemical and magnetic stability in solid state, organic solution and aqueous phase, and are promising for biomedical applications.

---



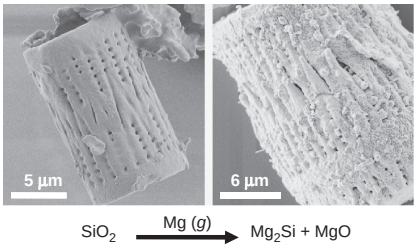


A nanostructured $Mg_2Si$ and MgO nanocomposite thermoelectric material is synthesized in the Mg gas-displacement solid state reduction of $SiO_2$ from diatomaceous earth. The resulting semiconducting $Mg_2Si$ nanostructures preserve the original diatom morphology, with nanosized grains at least down to the size of 30 nm.

---



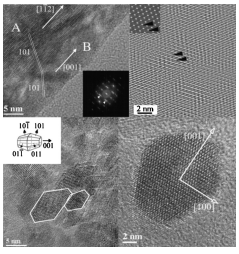

In the first part of this article, nonaqueous sol–gel routes to ternary metal oxide nanoparticles are briefly reviewed, followed by the discussion of the morphology-controlled synthesis of lanthanum hydroxide nanoparticles, and the appearance of an unprecedented superstructure in MnO nanoparticles. In the second part, doping experiments of $TiO_2$ with Fe and Co are presented, along with their characterization including magnetic measurements.

*Continued*

**Luminescence in colloidal $Mn^{2+}$-doped semiconductor nanocrystals**
Rémi Beaulac, Paul I. Archer and Daniel R. Gamelin
***page 1582***

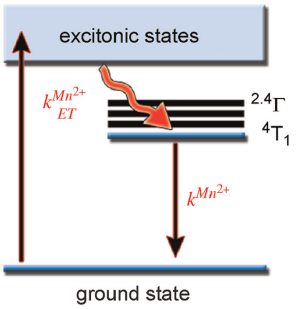


$Mn^{2+}$-doped semiconductor nanocrystals are organized into three major groups according to the location of various $Mn^{2+}$-related excited states relative to the energy gap of the host semiconductor nanocrystals. The positioning of these excited states gives rise to three distinct relaxation scenarios following photoexcitation.

---

**Multifunctional particles: Magnetic nanocrystals and gold nanorods coated with fluorescent dye-doped silica shells**
Andrew T. Heitsch, Danielle K. Smith, Reken N. Patel, David Ress and Brian A. Korgel
***page 1590***

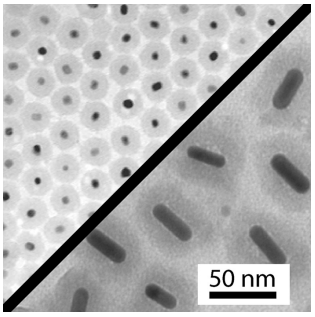


Colloidal gold nanorods and iron platinum and iron oxide nanocrystals were encapsulated with fluorescent dye-doped silica shells using a generic coating strategy. These heterostructures are promising contrast agents for dual-mode medical imaging. Their optical and magnetic properties were studied and are reported here.

---

**Controlling oriented aggregation using increasing reagent concentrations and trihalo acetic acid surfactants**
Anthony S. Ratkovich and R. Lee Penn
***page 1600***

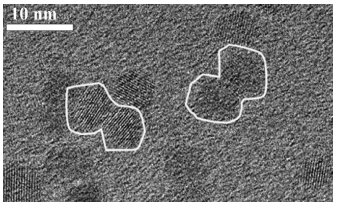


Zinc oxide particle growth from homogenous solutions prepared with isopropyl alcohol was monitored using *in situ* UV–vis spectroscopy. Oriented aggregation can be enhanced by increasing the number concentration of nanoparticles, which can be accomplished by increasing precursor concentrations. Furthermore, growth by oriented aggregation can be inhibited by employing an appropriate surfactant, such as trifluoroacetate.

**Synthesis of uniform-sized bimetallic iron–nickel phosphide nanorods**
Ki Youl Yoon, Youngjin Jang, Jongnam Park, Yosun Hwang, Bonil Koo, Je-Geun Park and Taeghwan Hyeon
***page 1609***

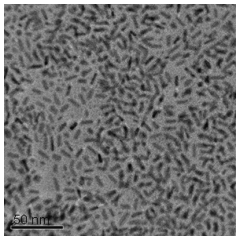


We synthesized uniform-sized nanorods of iron–nickel phosphides from thermal decomposition of metal–phosphine complexes. The magnetic studies showed that blocking temperature and coercive field depend on Ni content in the nanorods.

---

**Synthesis and catalytic properties of microemulsion-derived cerium oxide nanoparticles**
Emanuel Kockrick, Christian Schrage, Anett Grigas, Dorin Geiger and Stefan Kaskel
***page 1614***

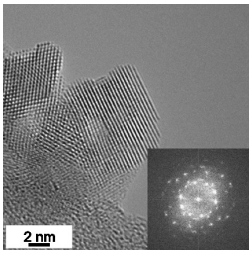


The synthesis of cerium dioxide nanoparticles using an inverse microemulsion technique and precipitation method was investigated using small angle X-ray scattering, dynamic light scattering and high-resolution transmission electron microscopy. Catalytic activity of ceria nanoparticles was tested in soot combustion reaction indicating size-dependent reactivity.

---

**Solid-state chemistry on a surface and in a beaker: Unconventional routes to transition metal chalcogenide nanomaterials**
Christopher L. Stender, Perumal Sekar and Teri W. Odom
***page 1621***

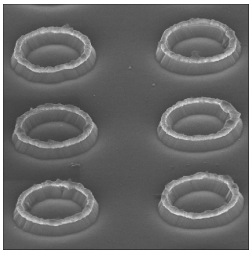

This paper describes how transition metal chalcogenide nanomaterials can be produced by two approaches. First, chemical nanofabrication—a combination of top-down patterning and bottom-up solid-state synthesis—was used to achieve control over the shape, size, and ordering of patterned nanomaterials. Second, a one-pot procedure using molecular precursors was developed to synthesize two-dimensional nanoplates and one-dimensional nanowires of conducting transition metal dichalcogenides.

**Alkyl-terminated crystalline Ge nanoparticles prepared from NaGe: Synthesis, functionalization and optical properties**
Xuchu Ma, Fengyi Wu and Susan M. Kauzlarich
*page 1628*

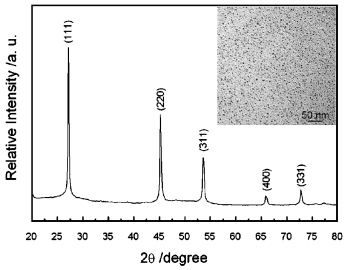


XRD pattern of crystalline Ge nanoparticles obtained by solid-state process and TEM image of alkyl-terminated crystalline Ge nanoparticles.

---

**GaN taper rods: Solid-phase synthesis, crystal defects, and optical properties**
Keyan Bao, Shuzhen Liu, Liang Shi, Shenglin Xiong, Jun Li, Xiaobo Hu, Jie Cao and Yitai Qian
*page 1634*

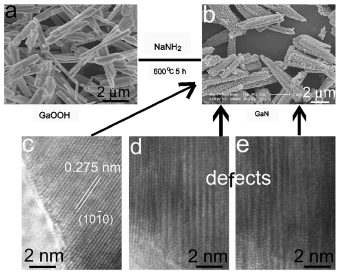


Wurtzite GaN taper rods assembled from highly oriented nanoparticles were synthesized using $NaNH_2$ and the as-synthesized GaOOH prismatic rods as reactants at 600 °C for 5 h. The lengths of the GaN taper rods are in the range of 4–6 μm and the diameters are about 0.5–1.5 μm. SAED patterns and HRTEM observations revealed that there were crystal defects in the GaN structure. The GaN taper rods displayed luminescence emission in the blue-violet region, which maybe related to crystal defects.

---

**Tomographic analysis of dilute impurities in semiconductor nanostructures**
D.E. Perea, E. Wijaya, J.L. Lensch-Falk, E.R. Hemesath and L.J. Lauhon
*page 1642*

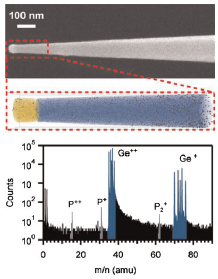


Scanning electron micrograph of a P-doped Ge nanowire including the Au catalyst tip (top). The corresponding 3D reconstruction (middle) and mass spectrum (bottom) of the boxed region produced via atom probe tomography. From the 3D reconstruction and mass spectrum, the concentration and distribution of dopants can be determined.

**Jingle-bell-shaped ferrite hollow sphere with a noble metal core: Simple synthesis and their magnetic and antibacterial properties**
Siheng Li, Enbo Wang, Chungui Tian, Baodong Mao, Zhenhui Kang, Qiuyu Li and Guoying Sun
*page 1650*

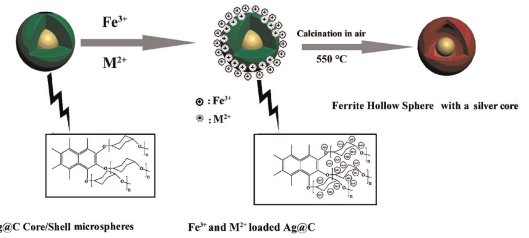


$MFe_2O_4$ ($M$ = Ni, Co, Mg, Zn) hollow spheres with a noble metal nanoparticle core were successfully prepared by using colloidal metal@C core–shell spheres as templates with no need of surface modification. The shell thickness and magnetic properties of the ferrite hollow spheres could be controlled by varying the synthetic parameters.

---

**Ordered mesoporous silica-based inorganic nanocomposites**
Qingqing Wang and Daniel F. Shantz
*page 1659*

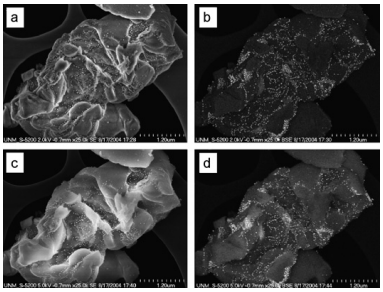


HAADF TEM image of gold nanoparticles in amine-functionalized MCM-41 (from Ref. [22]).

---

**Electrostatic characteristics of nanostructures investigated using electric force microscopy**
X.H. Qiu, G.C. Qi, Y.L. Yang and C. Wang
*page 1670*

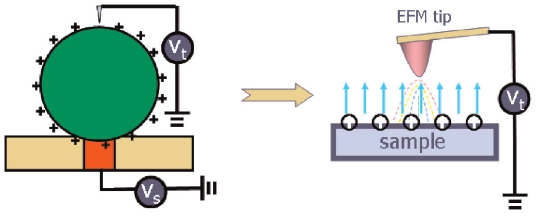


We review recent progress of electric force microscopy (EFM) and its applications in studying the electrical properties of nanostructures. A variety of important issues in EFM experimentation and theoretical modeling are discussed, with an emphasis on the ongoing efforts to improve the precision in quantitative measurements of charge density and dielectric properties of nanostructures.

*Continued*

**$K_4Nb_6O_{17}$-derived photocatalysts for hydrogen evolution from water: Nanoscrolls versus nanosheets**
Michael C. Sarahan, Elizabeth C. Carroll, Mark Allen, Delmar S. Larsen, Nigel D. Browning and Frank E. Osterloh
***page 1678***

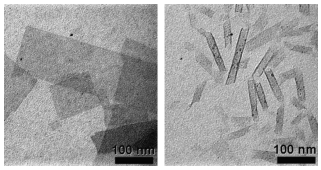


Nanosheets and nanoscrolls composed of individual niobate layers from $K_4Nb_6O_{17}$ are active for hydrogen generation from water and aqueous methanol under UV irradiation.

---

**Structure and dehydration of layered perovskite niobate with bilayer hydrates prepared by exfoliation/self-assembly process**
Yufeng Chen, Xinhua Zhao, Hui Ma, Shulan Ma, Gailing Huang, Yoji Makita, Xuedong Bai and Xiaojing Yang
***page 1684***

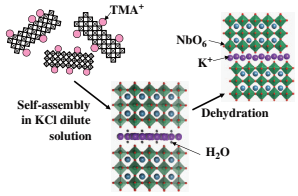


The structure of layered perovskite niobate $KCa_2Nb_3O_{10} \cdot xH_2O$ ($x = 1.3$) having a bilayers-hydrates interlayer, obtained via the exfoliation of an H-form precursor and the self-assembly of $Ca_2Nb_3O_{10}^-$ nanosheets, was first discussed in detail and determined to be tetragonal symmetry (*P4/mbm*). The dehydration resulted in the structural transformation to orthorhombic structure.

**Nanoscale structural order from the atomic pair distribution function (PDF): There's plenty of room in the middle**
Simon J.L. Billinge
***page 1695***

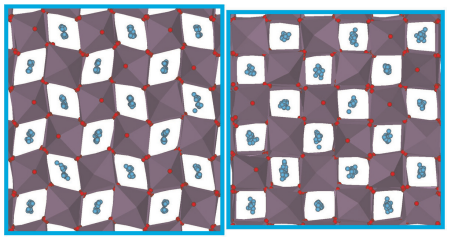

---

**The synthesis and characterization of new $[(BiSe)_{1.10}]_m[NbSe_2]_n$, $[(PbSe)_{1.10}]_m[NbSe_2]_n$, $[(CeSe)_{1.14}]_m[NbSe_2]_n$ and $[(PbSe)_{1.12}]_m[TaSe_2]_n$ misfit layered compounds**
Colby Heideman, Ngoc Nyugen, Jonathan Hanni, Qiyin Lin, Scott Duncombe, David C. Johnson and Paul Zschack
***page 1701***

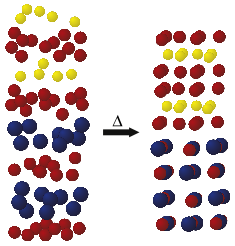


The synthesis and characterization of new $[(BiSe)_{1.10}]_m[NbSe_2]_n$, $[(PbSe)_{1.10}]_m[NbSe_2]_n$, $[(CeSe)_{1.14}]_m[NbSe_2]_n$, and $[(PbSe)_{1.12}]_m[TaSe_2]_n$ misfit layered compounds.




For a full and complete Guide for Authors, please refer to *J. Solid State Chem.,* Vol. 180, Issue 1, pp. *bmi–bmv*. The instructions can also be found at http://www.elsevier.com/wps/find/journaldescription.cws_home/622898/authorinstructions.

*Journal of Solid State Chemistry* has no page charges.